Cyanidin-3-O-β-glucoside inhibits lipopolysaccharide-induced inflammatory response in mouse mastitis model

Yunhe Fu, Zhengkai Wei, Ershun Zhou, Naisheng Zhang, and Zhengtao Yang[1]

Department of Clinical Veterinary Medicine, College of Veterinary Medicine, Jilin University, Changchun, Jilin Province 130062, People's Republic of China

Abstract Cyanidin-3-O-β-glucoside (C3G) (CAS number 7084-24-4), a typical anthocyanin pigment that exists in the human diet, has been reported to have anti-inflammatory properties. However, the effect of C3G on lipopolysaccharide (LPS)-induced mastitis and the molecular mechanisms have not been investigated. In this study, we detected the protective effects of C3G on a LPS-induced mouse mastitis model and investigated the molecular mechanisms in LPS-stimulated mouse mammary epithelial cells (MMECs). Our results showed that C3G could attenuate mammary histopathologic changes and myeloperoxidase activity, and inhibit TNF-α, interleukin (IL)-1β, and IL-6 production caused by LPS. Meanwhile, C3G dose-dependently inhibited TNF-α and IL-6 in LPS-stimulated MMECs. C3G suppressed LPS-induced nuclear factor-κB (NF-κB) and interferon regulatory factor 3 (IRF3) activation. Furthermore, C3G disrupted the formation of lipid rafts by depleting cholesterol. Moreover, C3G activated liver X receptor (LXR)-ABCG1-dependent cholesterol efflux. Knockdown of LXRα abrogated the anti-inflammatory effects of C3G. In conclusion, C3G has a protective effect on LPS-induced mastitis. The promising anti-inflammatory mechanisms of C3G are associated with upregulation of the LXRα-ABCG1 pathway which result in disrupting lipid rafts by depleting cholesterol, thereby suppressing toll-like receptor 4-mediated NF-κB and IRF3 signaling pathways induced by LPS.—Fu, Y., Z. Wei, E. Zhou, N. Zhang, and Z. Yang. **Cyanidin-3-O-β-glucoside inhibits lipopolysaccharide-induced inflammatory response in mouse mastitis model. *J. Lipid Res*. 2014.** 55: **1111–1119.**

Supplementary key words nuclear factor-κB • interferon regulatory factor 3 • toll-like receptor 4 • lipid raft • liver X receptor • ATP binding cassette transporter G1

Mastitis is a highly prevalent and important infectious disease and is responsible for severe production effects. Milk yield and composition can be affected, which results in impaired infant growth and development (1). Gram-negative bacteria are the most frequent causative agents of severe mastitis (2). Lipopolysaccharide (LPS), a main component of the outer membrane of gram-negative bacteria, has been identified as an important risk factor for mastitis (3). Toll-like receptor (TLR4) is the main receptor of LPS (4). Upon stimulation by LPS, TLR4 is recruited to lipid rafts and interacts with its adaptor molecules, resulting in nuclear factor-κB (NF-κB) and interferon regulatory factor 3 (IRF3) activation and cytokine production (5).

The liver X receptors (LXRs) are nuclear receptors that play central roles in the transcriptional control of lipid metabolism. Activation of LXRs induces expression of genes involved in cholesterol efflux, such as ABCA1 and ABCG1 (6). In addition to their function in lipid metabolism, LXRs have also been found to play an important role in inflammatory responses (7). Reports have shown that synthetic LXR agonists promote cholesterol efflux (the efflux of cholesterol from cells and total cell cholesterol, membrane cholesterol, and lipid raft cholesterol all go down) and inhibit inflammation (8). ABCA1 and ABCG1 are members of the ABC superfamily of transmembrane transporters that pump specific substrates across membranes (9). Both the ABCG1 and ABCA1 genes are expressed in numerous tissues and are highly activated by the nuclear receptor LXR. Activation of ABCA1 and ABCG1 can induce cholesterol efflux from the cell and downregulate lipid raft cholesterol levels (10). Lipid rafts are microdomains of the plasma membrane which are enriched in cholesterol and sphingolipids. They serve as a platform for signal transduction (11). Treatment with raft-disrupting drugs can inhibit the LPS-induced inflammatory response (12, 13).

This work was supported by grants from the National Natural Science Foundation of China (30972225 and 30771596) and the Research Fund for the Doctoral Program of Higher Education of China (20110061130010).

Manuscript received 22 January 2014 and in revised form 10 April 2014.

Published, JLR Papers in Press, April 14, 2014
DOI 10.1194/jlr.M047340

Abbreviations: C3G, cyanidin-3-O-β-glucoside; DEX, dexamethasone; GM1, Ganglioside M1; IL, interleukin; IRF3, interferon regulatory factor 3; LPS, lipopolysaccharide; LXR, liver X receptor; mAb, monoclonal Ab; MβCD, methyl-β-cyclodextrin; MMEC, mouse mammary epithelial cell; MPO, myeloperoxidase; MTT, 3-(4,5-dimethylthiazol-2-y1)-2,5-diphenyltetrazolium bromide; NF-κB, nuclear factor-κB; OD, optical density; RANTES, regulated upon activation normal T-cell expressed and secreted; TLR4, toll-like receptor 4.

[1]To whom correspondence should be addressed.
e-mail: yangzhengtao01@sina.com

Anthocyanins are a large group of phytochemicals occurring in a wide range of fruits and vegetables. Cyanidin-3-O-β-glucoside (C3G) (**Fig. 1**), one of the most investigated anthocyanins, has been reported to have anti-inflammatory effects. C3G was found to inhibit inflammatory mediators, including iNOS and COX-2 expression in LPS-stimulated THP-1 cells (14). It has been reported that C3G has specific inhibitory effects on NF-κB activation (15). However, the molecular mechanism of the anti-inflammatory actions of C3G in LPS-induced inflammatory response remains unclear. Although a number of studies have addressed the therapeutic potential of C3G (16, 17), its ability to protect against LPS-induced mastitis remains poorly understood. Herein, we report the preventive effects of C3G on LPS-induced mastitis in mice and elucidate the potential anti-inflammatory mechanism.

EXPERIMENTAL PROCEDURES

Reagents

C3G was purchased from the National Institute for the Control of Pharmaceutical and Biological Products (Beijing, China). Dexamethasone (DEX) (purity >99.6%) was purchased from Changle Pharmaceutical Co. (Xinxiang, Henan, China). Methyl-β-cyclodextrin (MβCD), DMSO, LPS (*Escherichia coli* 055:B5), and 3-(4,5-dimethylthiazol-2-y1)-2,5-diphenyltetrazolium bromide (MTT) were purchased from Sigma Chemical Co. (St. Louis, MO). DMEM and FBS were obtained from Hyclone. Mouse TNF-α, interleukin (IL)-6, and IL-1β ELISA kits were purchased from BioLegend (San Diego, CA). Mouse RANTES ELISA kits were purchased from R&D Systems (Minneapolis, MN). Mouse monoclonal Ab (mAb) phospho-NF-κB, mouse mAb NF-κB, mouse mAb phospho-IRF3, and rabbit mAb IRF3 were purchased from Cell Signaling Technology Inc. (Beverly, MA). LXRα and ABCG1 antibodies were purchased from Santa Cruz Biotechnology. HRP-conjugated goat anti-rabbit antibodies were provided by GE Healthcare (Buckinghamshire, UK). All other chemicals were of reagent grade.

Mouse model of LPS-induced mastitis

Seventy-two female mice were purchased from the Center of Experimental Animals of Baiqiuen Medical College of Jilin University (Jilin, China) 5–7 days after parturition. All animals were housed in microisolator cages and fed with standard laboratory chow and water ad libitum; the mice were kept at a temperature of 24 ± 1°C and a relative humidity of 40–80%. All experiments followed the guidelines for the care and use of laboratory animals published by the US National Institutes of Health. Both L4 (on the left) and R4 (on the right) abdominal mammary glands were infused with LPS using a 100 μl syringe with a 30-gauge blunt needle. Lactating mice were anesthetized by ethyl ether and put on their back under a binocular. The teats and the surrounding area were disinfected with 70% ethanol. LPS (10 μg dissolved in 50 μl sterile PBS) was infused into the mammary gland through the duct of the mammary gland (18).

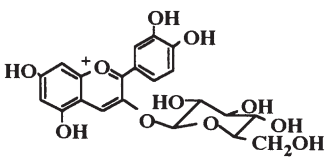

Fig. 1. Chemical structure of C3G.

Seventy-two female mice were randomly divided into six groups: the blank control group, the LPS group, the LPS + C3G groups (10, 20, or 40 mg/kg), and the LPS + DEX (5 mg/kg) group. The treatment groups were respectively administered 10, 20, and 40 mg/kg C3G ip at 1 h before and 12 h after LPS infusion based on our preliminary experiment. The DEX group was administered 5 mg/kg DEX ip at 1 h before and 12 h after LPS infusion. The blank control group and LPS group were supplied with an equal volume of distilled water ip. At 24 h after LPS inoculation, the mice were euthanized with CO_2 inhalation and then the four pairs of mammary glands were collected and stored at −80°C until analysis.

Histopathologic evaluation of the mammary tissue

The mammary tissues were collected and fixed with 10% buffered formalin, imbedded in paraffin, and sliced. After hematoxylin and eosin staining, pathological changes of the mammary tissues were observed under a light microscope.

Myeloperoxidase activity analysis

Myeloperoxidase (MPO) activity represents the parenchymal infiltration of neutrophils and macrophages. MPO activity in homogenates of mammary tissue was determined using test kits purchased from Nanjing Jiancheng Bioengineering Institute (China) according to the instructions.

Cell culture and treatment

Mouse mammary epithelial cells (MMECs) were prepared as previously described. Briefly, the mammary glands from pregnant female mice were minced and digested at 37°C with a collagenase I/II/trypsin mixture (Invitrogen, Carlsbad, CA). Undissociated tissues and debris were removed after filtration. Then the cells were collected by centrifugation at 250 *g* for 5 min three times. Cell pellets were resuspended in DMEM/F12 containing 10% FCS and incubated for 1 h at 37°C, and then the supernatant was collected. This step was repeated three times to clear away fibroblasts. After the last incubation, cells were resuspended in DMEM/F12 containing 10% FCS, 0.5% transferrin, 0.1% T3, and 0.5% EGF and cultured at 37°C with 5% CO_2. Medium was changed once every 48 h. In all experiments, MMECs were incubated in the presence or absence of various concentrations of C3G that was always added 12 h prior to LPS (0.1 μg/ml) treatment.

MTT assay for cell viability

Cell viability was determined by MTT assay. In brief, 1×10^4 MMECs were isolated and seeded in 96-well plates, then the cells were treated with 50 μl of C3G at different concentrations (0–100 μM) for 1 h, followed by stimulation with 50 μl LPS. After 18 h of LPS stimulation, 20 μl MTT (5 mg/ml) was added to each well, and the cells were further incubated for an additional 4 h. The supernatant was removed and the formation of formazan was resolved with 150 μl/well of DMSO. The optical density (OD) was measured at 570 nm on a microplate reader (TECAN, Austria).

ELISA assay

The levels of inflammatory cytokines, TNF-α, IL-1β, IL-6, and RANTES, were measured by ELISA kits according to the manufacturer's instructions (BioLegend).The OD of the microplate was read at 450 nm.

Western blot analysis

Total proteins from cells were extracted by mammalian protein extraction reagent (M-PER, Thermo). Briefly, culture medium

was carefully removed from cells. Then, 200 μl M-PER reagent was added to the 6-well plate and shaken gently for 5 min. The lysate was collected and transferred to a microcentrifuge tube and centrifuged at 14,000 *g* for 7 min to pellet the cell debris. Then the supernatant was transferred for analysis.

Protein concentration was determined through the BCA method. Equal amounts of protein were loaded in each well and separated by 10% SDS-PAGE, which subsequently was transferred onto a polyvinylidene difluoride membrane. The membrane was blocked for 2 h with 5% skim milk in TBST on the shaker at room temperature and then washed three times (10 min each) with Tri-Tween buffered saline [20 mM Tris-HCl buffer (pH 7.6), 137 mM NaCl, and 0.05% Tween 20]. The membrane was placed on primary antibody diluted at a 1:1,000 proportion in diluent buffer [5% (w/v) BSA and 0.1% Tween 20 in TBS] and incubated overnight at 4°C on the shaker. Subsequently, the membrane was washed with PBS-T followed by incubation with the secondary antibody conjugated with HRP at room temperature for 1 h. The membrane was again washed three times (10 min each), as above, and finally the results were generated by using an ECL Western blotting kit.

Isolation of lipid rafts

Lipid rafts were isolated as described previously (19). Briefly, MMECs were lysed in ice-cold MBS buffer [25 mM MES (pH 6.5), 150 mM NaCl, 1 mM Na_3VO_4, 1% Triton X-100, and protease inhibitors]. Lysates were mixed with 4 ml of 40% sucrose by mixing with 2 ml of 80% sucrose and overlaid with 4 ml of 35% sucrose and 4 ml of 5% sucrose in MBS buffer. Samples were ultracentrifuged at 39,000 rpm for 18 h and fractionated into 12 subfractions. The translocation of TLR4 to lipid rafts was measured by Western blot analysis.

Quantification of cholesterol levels in lipid rafts of MMECs

Lipid rafts were isolated as described above. The cholesterol level of lipid rafts was assayed by gas-liquid chromatography as previously described (20).

Cholesterol replenishment experiment

MMECs were treated with culture medium alone or medium containing C3G (10, 20, or 40 μM), or MβCD (10 mM) at 37°C for 60 min. Subsequently, the cells were washed with PBS and incubated with medium alone or medium containing water-soluble cholesterol (84 μg/ml) for 30 min (21). The cells were exposed to LPS. The translocation of TLR4 to lipid rafts was analyzed as mentioned above.

LXR gene assay

For LXR activation studies, 0.75 μg of LXRE-driven luciferase reporter vector (LXRE-tk-Luc) and 0.75 μg of β-galactosidase control vector (Promega) were used. The MMECs were transfected with vectors using FuGENE HP transfection reagent (Roche Applied Science, Indianapolis, IN) according to the manufacturer's instructions. Six hours after transfection, cells were treated with C3G for 12 h. The β-galactosidase enzyme activity was determined using the β-galactosidase enzyme system (Promega) according to the manufacturer's instructions. Luciferase activity was normalized by β-galactosidase activity.

Transient transfection of siRNA against LXRα

The plasmid containing siRNA against LXRα (si-LXRα; ON-TARGETplus SMART pool), nontargeting siRNA (si-control), and the DharmaFECT transfection reagent were purchased from Thermo Scientific Dharmacon (USA). si-LXRα and si-control stock solutions (20 μM) were diluted with diethyl pyrocarbonate water to form 5 μM solutions. The DharmaFECT transfection reagent was mixed with 5 μM si-LXRα or si-control, incubated for 20 min, and then added to the culture medium at a final concentration of 25 μM. The MMECs were incubated with si-LXRα and si-control for 48 h.

Statistical analysis

All data are expressed as mean ± SEM. The differences among the various experimental groups were analyzed by one-way ANOVA. $P < 0.05$ was considered to be statistically significant.

RESULTS

C3G improved the LPS-induced histopathologic changes

Histopathologic changes of mammary gland tissues from each experimental group were examined after hematoxylin and eosin staining. There was no inflammatory reaction in the control group (**Fig. 2A**). Compared with the control group, apparent histopathologic changes could be seen in

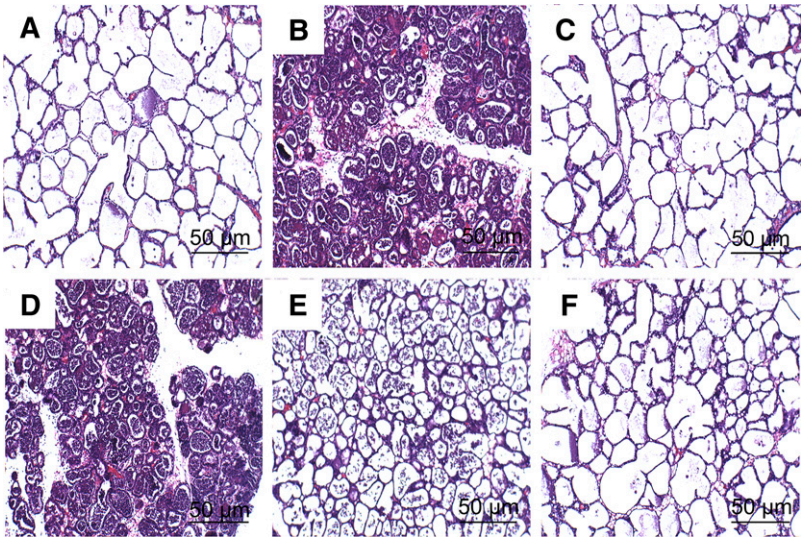

Fig. 2. Histopathologic sections of mammary gland tissues (hematoxylin and eosin, ×100), mammary gland tissue of control group (A), LPS group (B), LPS group (C), LPS + C3G (10 mg/kg) (D), LPS + C3G (20 mg/kg) (E), and LPS + C3G (40 mg/kg) (F).

the LPS group, represented by thickening of the alveolar wall, interstitial patchy hemorrhage, hyperemia, edema, and the extensive existence of inflammatory cells in alveolar spaces (Fig. 2B). In the LPS + C3G groups with the dose of 10 (Fig. 2D), 20 (Fig. 2E), and 40 mg/kg (Fig. 2F), LPS-induced histopathologic changes were markedly attenuated in a dose-dependent manner. Treatment with DEX (5 mg/kg, Fig. 2C) also significantly reduced the injury of mammary gland tissues compared with the LPS group.

Effects of C3G on the MPO activity

As shown in **Fig. 3**, LPS significantly increased the MPO activity in mammary tissue ($P < 0.01$) compared with the control group. MPO activity was reduced in the treatment groups, especially the treatment groups of 20 mg/kg and 40 mg/kg which had markedly decreased MPO activity in comparison with the LPS group ($P < 0.05$ and $P < 0.01$).

C3G decreased the levels of pro-inflammatory cytokines

The levels of pro-inflammatory cytokines, TNF-α, IL-1β and IL-6, were measured by ELISA. Compared with the control group, LPS significantly increased the levels of TNF-α, IL-1β, and IL-6. In contrast, these increases induced by LPS were significantly decreased by C3G (**Fig. 4**).

Effects of C3G on cell viability

The potential cytotoxicity of C3G was evaluated by the MTT assay after incubating cells for 18 h in the absence or presence of LPS; the result showed that cell viabilities were not affected by the C3G at the concentrations used (10, 20, or 40 μM) (**Fig. 5**). Thus, the effects of C3G on MMECs were not attributable to cytotoxic effects.

Effects of C3G on cytokine production in LPS-stimulated MMECs

The expression of TNF-α, IL-6, and RANTES was detected by ELISA. The results showed that C3G suppressed TNF-α, IL-6, and RANTES production in LPS-stimulated MMECs in a dose-dependent manner (**Fig. 6**).

C3G suppresses LPS-induced NF-κB and IRF3 activation

NF-κB and IRF3 play a critical role in regulating of inflammatory cytokine expression. Once stimulated by LPS, NF-κB and IRF3 phosphorylation activates these proteins (5). In this study, we detect whether the inhibition of inflammatory response by C3G is mediated through the NF-κB and IRF3 pathways. NF-κB and IRF3 protein were determined by Western blotting. The results showed that C3G significantly inhibits the phosphorylation of NF-κB and IRF3 (**Fig. 7**).

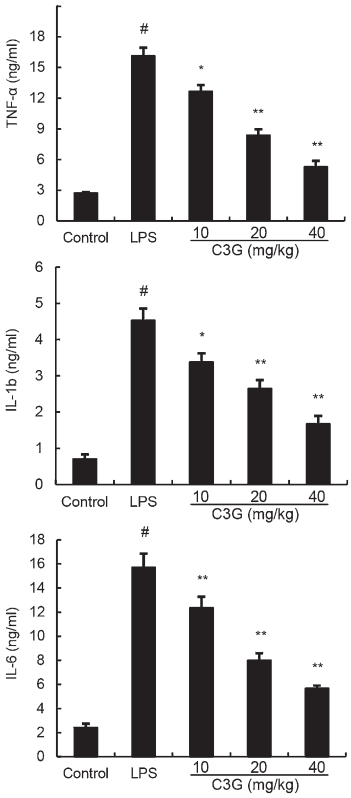

Fig. 4. The levels of TNF-α, IL-1β, and IL-6 in the homogenate of mouse mammary tissues including control group, LPS group, and treatment groups with C3G (10, 20, or 40 mg/kg). Data represent the contents of 1 g mammary tissue, and are presented as mean ± SEM (n = 6). $^{\#}P < 0.01$ significantly different from control group; $^{*}P < 0.05$ and $^{**}P < 0.01$ significantly different from LPS group.

C3G inhibits translocation of TLR4 to lipid rafts

Lipid rafts play an important role in the TLR4 signaling pathway. LPS induced TLR4 to recruit into lipid

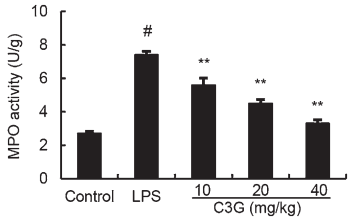

Fig. 3. Effects of C3G on MPO activity in mammary gland of LPS-induced mastitis. Mice were given an ip injection of C3G (10, 20, or 40 mg/kg) 1 h before and 12 h after LPS instillation, respectively. MPO activity was determined at 24 h after LPS administration. The values presented are the mean ± SEM (n = 6). $^{\#}P < 0.01$ significantly different from control group; $^{**}P < 0.01$ significantly different from LPS group.

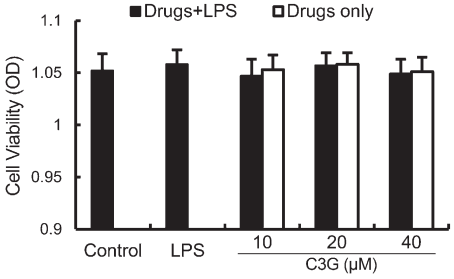

Fig. 5. Effect of C3G on the cell viability of MMECs. Cells were cultured with different concentrations of C3G (0–100 μM) in the absence or presence of 0.1 μg/ml LPS for 24 h. The cell viability was determined by MTT assay. The values presented are the mean ± SEM of three independent experiments.

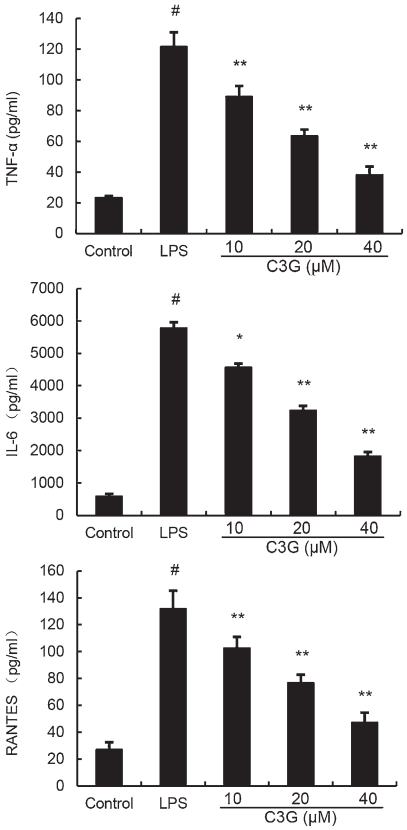

Fig. 6. C3G inhibits LPS-induced cytokine production in a dose-dependent manner. MMECs were treated with 0.1 μg/ml LPS in the absence or presence of C3G (10, 20, or 40 μM) for 24 h. Levels of TNF-α, RANTES, and IL-6 in culture supernatants were measured by ELISA. The data presented are the mean ± SEM of three independent experiments and differences between mean values were assessed by ANOVA. $^{\#}P < 0.05$ versus control group; $^{*}P < 0.05$ and $^{**}P < 0.01$ versus LPS group.

rafts (22). To further address the potential anti-inflammatory effects of C3G, we determined the effects of C3G on the translocation of TLR4 to lipid rafts. We isolated raft fractions and examined the translocation of TLR4 by Western blotting. As shown in **Fig. 8A**, GM1 was lost from the rafts in C3G-treated cells, suggesting that C3G could destroy lipid rafts. The results also showed that LPS stimulation induced localization of TLR4 to raft fractions. This effect was prevented by pretreatment with C3G or MβCD (Fig. 8A). The results (Fig. 8B) showed that the cholesterol amounts in rafts were decreased by C3G or MβCD. Meanwhile, the cholesterol amounts in total fractions were also decreased by C3G or MβCD.

C3G decreases lipid raft cholesterol levels in MMECs

Lipid rafts are plasma membrane microdomains that contain high concentrations of cholesterol and glycosphingolipids. Studies have shown that treatment with raft-disrupting drugs can inhibit TLR4 translocation into lipid rafts and LPS-induced NF-κB activation and TNF-α production in macrophages (23). Thus, we determined whether C3G decreased cholesterol levels of lipid rafts in MMECs. As shown in **Fig. 9**, the cholesterol levels of lipid rafts were decreased by C3G in a dose-dependent manner.

Cholesterol replenishment prevents the anti-inflammatory effect of C3G

Cholesterol replenishment experiments were carried out to detect the anti-inflammatory mechanism of C3G. As shown in **Fig. 10**, the inhibition effect of C3G on LPS-induced cytokines was abolished.

C3G upregulates the expression of LXRα and ABCG1 in MMECs

LXRα plays an important role in cholesterol homeostasis by regulating the sensors of cholesterol levels in cells. Activation of LXRα induces expression of genes involved in cholesterol efflux, such as ABCG1. In this study, we performed a luciferase reporter gene assay to test whether C3G could enhance transcriptional activity of LXRα. As

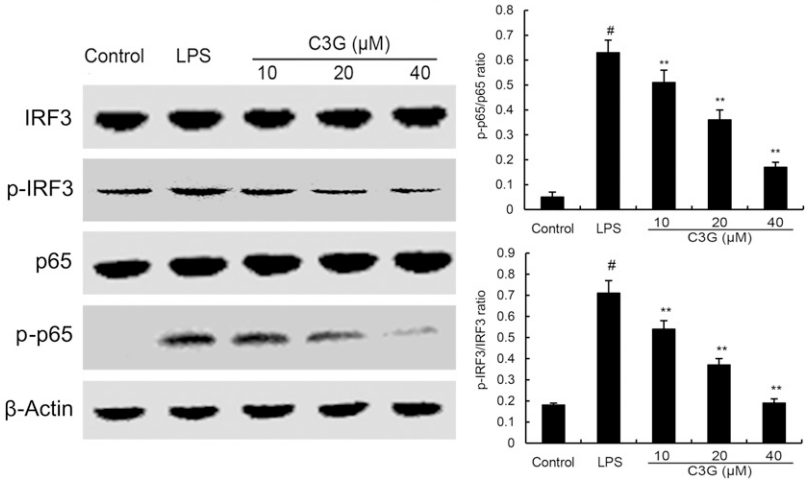

Fig. 7. C3G inhibits LPS-induced NF-κB and IRF3 phosphorylation. MMECs were preincubated with C3G (10, 20, or 40 μM) for 12 h and then treated with 0.1 μg/ml LPS for 1 h. Protein samples were analyzed by Western blot with specific antibodies. $^{\#}P < 0.05$ versus control group; $^{**}P < 0.01$ versus LPS group.

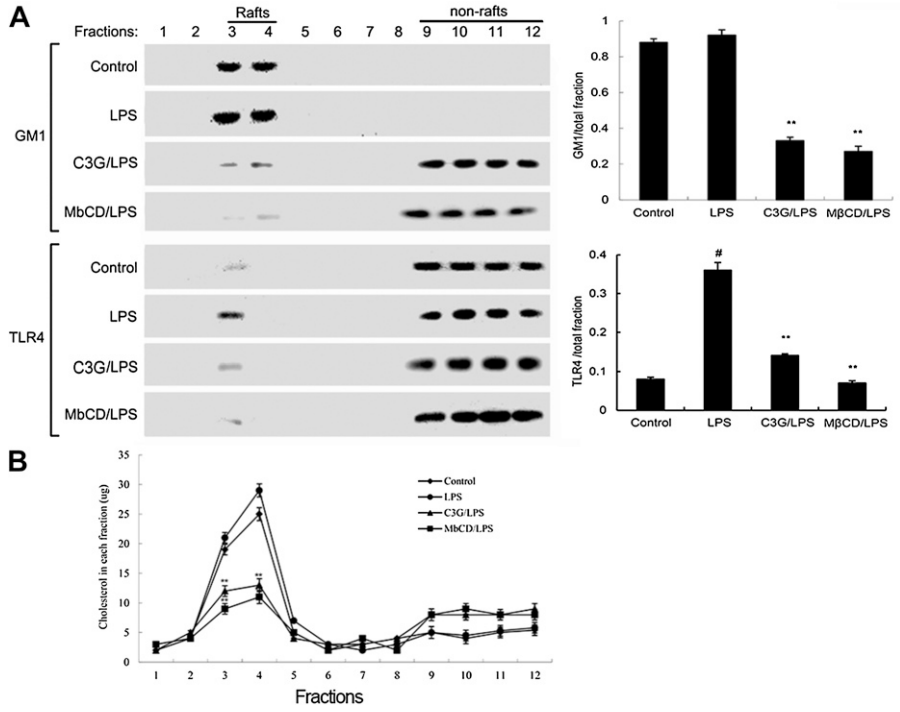

Fig. 8. A: The recruitment of TLR4 to lipid rafts was inhibited by C3G. MMECs were pretreated with C3G or MβCD, followed by treatment with 0.1 μg/ml LPS. The cells were lysed and subjected to discontinuous sucrose density gradient centrifugation as described in the Experimental Procedures. The fractions were analyzed by Western blotting using CTxB conjugated to HRP (GM1) or anti-TLR4 primary antibody. Fractions 3 and 4 correspond to lipid rafts. Representative blots of three separate experiments are shown. GM-1 and TLR4 content of macrophage lipid rafts was calculated as the amount of GM1 and the amount of TLR4 per total fractions. B: Cholesterol levels in each fraction were measured. The values presented are the mean ± SEM of three independent experiments and differences between mean values were assessed by Students's *t*-test. $^{\#}P < 0.05$ versus control group; $^{**}P < 0.01$ versus LPS group.

shown in **Fig. 11A**, C3G dose-dependently increased expression of the LXR luciferase reporter gene. Meanwhile, the expression of LXRα and ABCG1 were detected by Western blotting. As shown in Fig. 11B, C3G upregulated the expression of LXRα and ABCG1 in a dose-dependent manner.

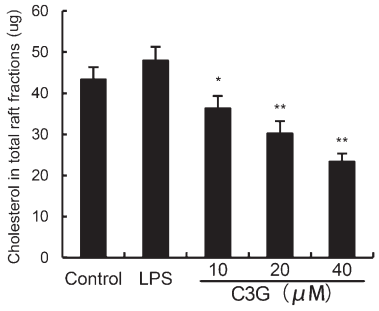

Fig. 9. Effects of C3G on lipid raft cholesterol levels. MMECs were treated with C3G (10, 20, or 40 μM) for 12 h. Lipid raft cholesterol levels in the total raft fractions, as depicted in Fig. 8, were measured by gas-liquid chromatography. The values presented are the mean ± SEM of three independent experiments and differences between mean values were assessed by Students's *t*-test ($^{*}P < 0.05$, $^{**}P < 0.01$).

Knockdown of LXRα abrogated the effects of C3G on lipid raft cholesterol levels, and LPS induced inflammatory response in MMECs

To detect whether the anti-inflammatory effects of C3G is LXRα dependent, LXRα was silenced in MMECs by its specific siRNA. When LXRα was silenced, the effects of C3G on cholesterol levels and cytokines expression induced by LPS were reversed (**Fig. 12**) (**Fig. 13**).

DISCUSSION

Bovine mastitis is a highly prevalent and important infectious disease of dairy cattle. It is characterized by mammary gland edema, mammary alveolar damage, and inflammatory cell infiltration. LPS, a main component of the outer membrane of gram-negative bacteria, has been identified as an important risk factor for mastitis (24). C3G, a typical anthocyanin pigment that exists in the human diet, has been reported to have anti-inflammatory properties. In the present study, we detected the effects of C3G on LPS-induced mastitis. The results showed that C3G obviously decreased mammary gland injury and MPO activity. These results indicated that C3G had a protective effect of LPS-induced mastitis.

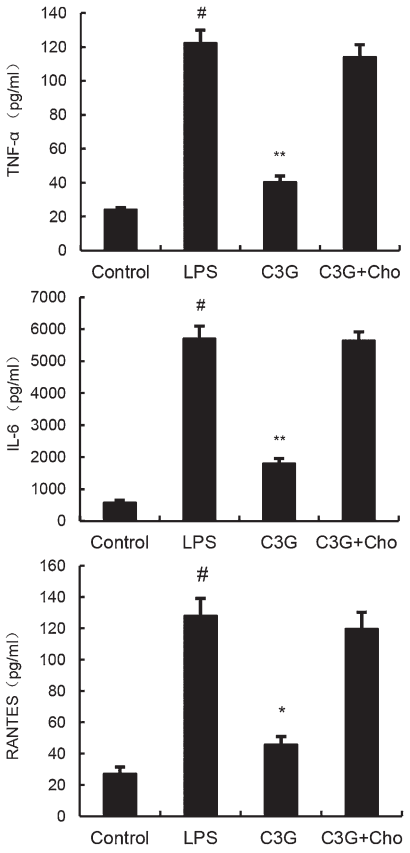

Fig. 10. Cholesterol (Cho) replenishment prevents the anti-inflammatory effect of C3G. MMECs were treated with culture medium alone or medium containing C3G (10, 20, or 40 μM) or MβCD (10 mM) at 37°C for 60 min. Subsequently the cells were washed with PBS and incubated with medium alone or medium containing water-soluble cholesterol (84 μg/ml) for 30 min. Cells were treated with 0.1 μg/ml LPS for 24 h. Levels of TNF-α, RANTES, and IL-6 in culture supernatants were measured by ELISA. The data presented are the mean ± SEM of three independent experiments and differences between mean values were assessed by ANOVA. $^{\#}P < 0.05$ versus control group; $^{*}P < 0.05$ and $^{**}P < 0.01$ versus LPS group.

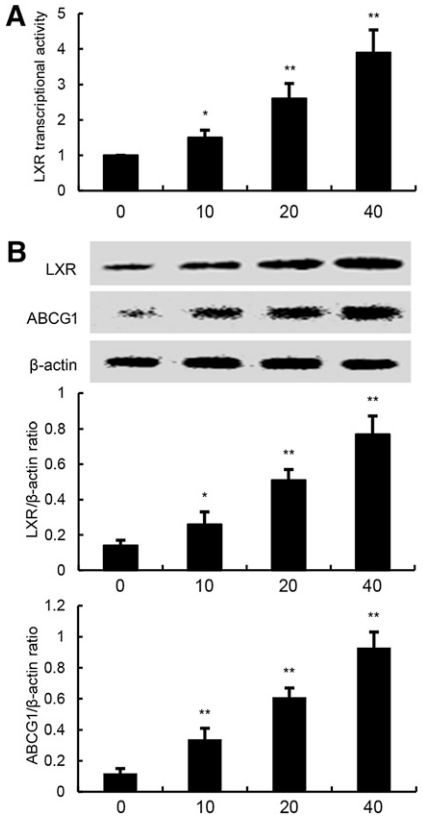

Fig. 11. Effects of C3G on LXR transcriptional activity and LXRα and ABCG1 expression. A: Cells were transfected with LXRE-driven luciferase reporter vector (LXRE-tk-Luc) and β-galactosidase control vector (Promega). Six hours later, cells were treated with C3G for 12 h. Relative luciferase activity was determined by normalization with β-galactosidase activity ($^{*}P < 0.05$, $^{**}P < 0.01$). B: Effects of C3G on LXRα and ABCG1 expression. Cells were treated with C3G (10, 20, or 40 μM) for 12 h. Protein samples were analyzed by Western blot with specific antibodies. β-Actin was used as a control. The values presented are the mean ± SEM of three independent experiments and differences between mean values were assessed by Students's *t*-test ($^{*}P < 0.05$, $^{**}P < 0.01$).

Mammary epithelial cells directly contact with the invading pathogens and play an important role in upper immunity (25). They recognize the pathogen-associated molecular patterns of invading pathogens via pattern recognition receptors such as TLRs, and induce the production of cytokines. Thus, we used the mammary epithelial cells to investigate the mechanism of C3G on LPS-induced mastitis in vitro. Cytokines, an important group of inflammatory mediators, play an important role in the process of mastitis (26). Elevated TNF-α and IL-6 were observed in LPS-induced mastitis (3, 27). These cytokines, as well as other inflammatory mediators, initiate, amplify, and perpetuate the inflammatory response in mastitis. In this study, we found that C3G inhibited the production of TNF-α and IL-6 in a dose-dependent manner. It has been reported that the expression of cytokines is modulated by NF-κB and IRF3. In this study, we investigated the effects of C3G on LPS-induced NF-κB and IRF3 activation. The results showed that C3G inhibited LPS-induced cytokine production by preventing NF-κB and IRF3 phosphorylation. However, the molecular targets of C3G have not been identified.

TLR4 is the major receptor for LPS. LPS signaling is initiated by binding to TLR4, leading to activation of downstream targets. Recently, reports have shown that lipid rafts play an important role in the TLR4 signaling pathway (12). Lipid rafts provide platforms for the formation of receptor complexes and play fundamental roles in signaling transduction. Upon stimulation by LPS, TLR4 is recruited to lipid rafts and induces downstream signaling activation (28). To further clarify the mechanism of C3G on LPS-induced inflammatory response, we investigated the effects of C3G on cholesterol levels in lipid rafts. The results showed that C3G could decrease the levels of cholesterol in lipid rafts. Meanwhile, our cholesterol replenishment

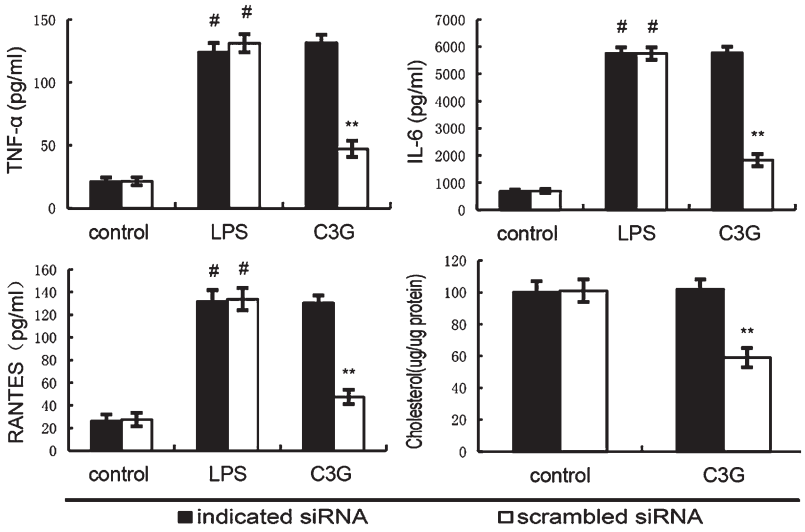

Fig. 12. Knockdown of LXRα abrogates the effects of C3G on lipid raft cholesterol levels, and LPS induces inflammatory response in MMECs. Cells were transfected with a siRNA specific for LXRα, or a scrambled siRNA (negative control) as indicated. Then the cells were treated with C3G (40 μM) for 12 h. Lipid raft cholesterol levels were detected. Meanwhile, the cells were treated with C3G (40 μM) for 12 h and stimulated by 0.1 μg/ml LPS for 24 h. Levels of TNF-α, RANTES, and IL-6 in culture supernatants were measured by ELISA. The data presented are the mean ± SEM of three independent experiments and differences between mean values were assessed by Students's *t*-test. $^{\#}P < 0.05$ versus control group; $^{**}P < 0.01$ versus LPS group.

results confirmed that after cholesterol replenishment, the inhibition effect of C3G on LPS-induced cytokines was abolished. Overall, our results demonstrated that C3G disrupted lipid rafts by depleting cholesterol and inhibiting LPS-induced inflammatory responses.

LXRα and LXRβ are members of the nuclear receptor superfamily that regulates cholesterol homeostasis (29). LXRs regulate intracellular cholesterol levels through mediating the expression of ABCG1 (30). ABCG1 is known to play an important role in cholesterol and oxysterol efflux (31, 32). To investigate the reason that C3G decreased the cholesterol levels in lipid rafts, we detected the effects of C3G on LXRα and ABCG1 activation. Our results showed that C3G increased LXRα and ABCG1 expression. These results suggest that C3G activates the LXRα-ABCG1 pathway by mediating cholesterol efflux to reduce lipid raft cholesterol content. To further confirm the involvement of the LXRα-ABCG1 pathway in the anti-inflammatory effect of C3G on mammary epithelial cells, LXRα was silenced by siRNA. We showed that when LXRα was silenced, the effects of C3G on ABCG1 expression, membrane cholesterol levels, and expression of cytokines induced by LPS were reversed. The present results obtained from LXRα knockdown support the critical role of the LXRα-ABCG1 pathway in the anti-inflammatory effects of C3G.

In conclusion, the studies demonstrate that C3G inhibits LPS-induced inflammatory cytokine production. The promising anti-inflammatory effect of C3G on LPS-stimulated primary MMECs is associated with upregulation of the LXRα-ABCG1 pathway, thereby suppressing TLR4-mediated NF-κB and IRF3 signaling pathways induced by LPS.

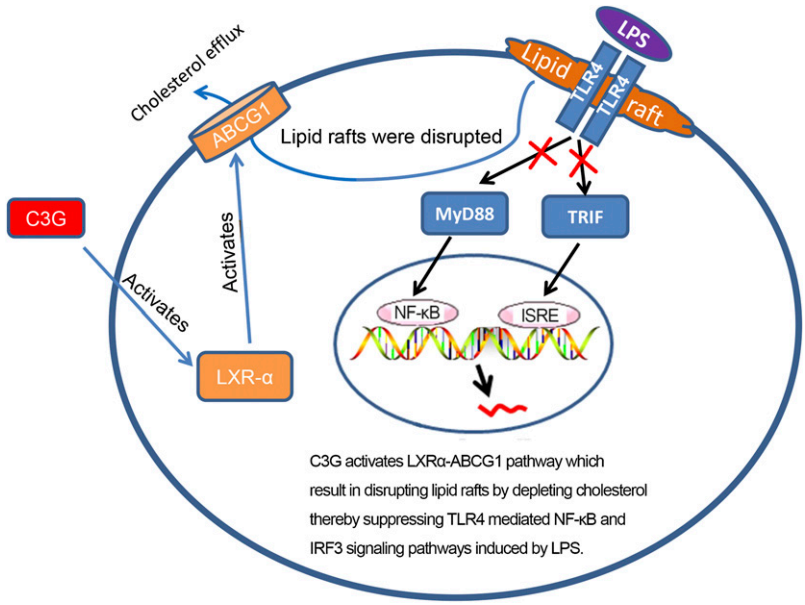

Fig. 13. Anti-inflammatory mechanism of C3G is associated with upregulation of the LXRα-ABCG1 pathway which results in disrupting lipid rafts by depleting cholesterol, thereby suppressing the TLR4-mediated NF-κB and IRF3 signaling pathways induced by LPS.

REFERENCES

1. Tankeyoon, M., N. Dusitsin, S. Chalapati, S. Koetsawang, S. Saibiang, M. Sas, J. J. Gellen, O. Ayeni, R. Gray, A. Pinol, et al. 1984. Effects of hormonal contraceptives on milk volume and infant growth. WHO Special Programme of Research, Development and Research Training in Human Reproduction Task force on oral contraceptives. *Contraception.* **30:** 505–522.
2. Fox, L. K. 2009. Prevalence, incidence and risk factors of heifer mastitis. *Vet. Microbiol.* **134:** 82–88.
3. Schmitz, S., M. W. Pfaffl, H. H. D. Meyer, and R. M. Bruckmaier. 2004. Short-term changes of mRNA expression of various inflammatory factors and milk proteins in mammary tissue during LPS-induced mastitis. *Domest. Anim. Endocrinol.* **26:** 111–126.
4. Hoshino, K., O. Takeuchi, T. Kawai, H. Sanjo, T. Ogawa, Y. Takeda, K. Takeda, and S. Akira. 1999. Cutting edge: Toll-like receptor 4 (TLR4)-deficient mice are hyporesponsive to lipopolysaccharide: evidence for TLR4 as the Lps gene product. *J. Immunol.* **162:** 3749–3752.
5. Fitzgerald, K. A., D. C. Rowe, B. J. Barnes, D. R. Caffrey, A. Visintin, E. Latz, B. Monks, P. M. Pitha, and D. T. Golenbock. 2003. LPS-TLR4 signaling to IRF-3/7 and NF-kappaB involves the toll adapters TRAM and TRIF. *J. Exp. Med.* **198:** 1043–1055.
6. Ulven, S. M., K. T. Dalen, J. A. Gustafsson, and H. I. Nebb. 2004. Tissue-specific autoregulation of the LXRalpha gene facilitates induction of apoE in mouse adipose tissue. *J. Lipid Res.* **45:** 2052–2062.
7. Joseph, S. B., A. Castrillo, B. A. Laffitte, D. J. Mangelsdorf, and P. Tontonoz. 2003. Reciprocal regulation of inflammation and lipid metabolism by liver X receptors. *Nat. Med.* **9:** 213–219.
8. Zelcer, N., and P. Tontonoz. 2006. Liver X receptors as integrators of metabolic and inflammatory signaling. *J. Clin. Invest.* **116:** 607–614.
9. Stefková, J., R. Poledne, and J. A. Hubácek. 2004. ATP-binding cassette (ABC) transporters in human metabolism and diseases. *Physiol. Res.* **53:** 235–243.
10. Zhu, X., J. S. Owen, M. D. Wilson, H. Li, G. L. Griffiths, M. J. Thomas, E. M. Hiltbold, M. B. Fessler, and J. S. Parks. 2010. Macrophage ABCA1 reduces MyD88-dependent Toll-like receptor trafficking to lipid rafts by reduction of lipid raft cholesterol. *J. Lipid Res.* **51:** 3196–3206.
11. Szabo, G., A. Dolganiuc, Q. Dai, and S. B. Pruett. 2007. TLR4, ethanol, and lipid rafts: a new mechanism of ethanol action with implications for other receptor-mediated effects. *J. Immunol.* **178:** 1243–1249.
12. Olsson, S., and R. Sundler. 2006. The role of lipid rafts in LPS-induced signaling in a macrophage cell line. *Mol. Immunol.* **43:** 607–612.
13. Triantafilou, M., K. Miyake, D. T. Golenbock, and K. Triantafilou. 2002. Mediators of innate immune recognition of bacteria concentrate in lipid rafts and facilitate lipopolysaccharide-induced cell activation. *J. Cell Sci.* **115:** 2603–2611.
14. Wang, Q., M. Xia, C. Liu, H. Guo, Q. Ye, Y. Hu, Y. Zhang, M. Hou, H. Zhu, J. Ma, et al. 2008. Cyanidin-3-O-beta-glucoside inhibits iNOS and COX-2 expression by inducing liver X receptor alpha activation in THP-1 macrophages. *Life Sci.* **83:** 176–184.
15. Zhang, Y., F. Lian, Y. Zhu, M. Xia, Q. Wang, W. Ling, and X. D. Wang. 2010. Cyanidin-3-O-beta-glucoside inhibits LPS-induced expression of inflammatory mediators through decreasing I kappa B alpha phosphorylation in THP-1 cells. *Inflamm. Res.* **59:** 723–730.
16. Wang, D., M. Xia, S. Gao, D. Li, Y. Zhang, T. Jin, and W. Ling. 2012. Cyanidin-3-O-β-glucoside upregulates hepatic cholesterol 7α-hydroxylase expression and reduces hypercholesterolemia in mice. *Mol. Nutr. Food Res.* **56:** 610–621.
17. Wang, Y., Y. H. Zhang, X. M. Wang, Y. Liu, and M. Xia. 2012. Supplementation with cyanidin-3-O-β-glucoside protects against hypercholesterolemia-mediated endothelial dysfunction and attenuates atherosclerosis in apolipoprotein E-deficient mice. *J. Nutr.* **142:** 1033–1037.
18. Li, D., N. Zhang, Y. Cao, W. Zhang, G. Su, Y. Sun, Z. Liu, F. Li, D. Liang, B. Liu, et al. 2013. Emodin ameliorates lipopolysaccharide-induced mastitis in mice by inhibiting activation of NF-kappa B and MAPKs signal pathways. *Eur. J. Pharmacol.* **705:** 79–85.
19. Kim, H. P., X. Wang, F. Galbiati, S. W. Ryter, and A. M. Choi. 2004. Caveolae compartmentalization of heme oxygenase-1 in endothelial cells. *FASEB J.* **18:** 1080–1089.
20. Zhu, X., J. Y. Lee, J. M. Timmins, J. M. Brown, E. Boudyguina, A. Mulya, A. K. Gebre, M. C. Willingham, E. M. Hiltbold, N. Mishra, et al. 2008. Increased cellular free cholesterol in macrophage-specific Abca1 knock-out mice enhances pro-inflammatory response of macrophages. *J. Biol. Chem.* **283:** 22930–22941.
21. Meng, G., Y. Liu, C. Lou, and H. Yang. 2010. Emodin suppresses lipopolysaccharide-induced pro-inflammatory responses and NF-κB activation by disrupting lipid rafts in CD14-negative endothelial cells. *Br. J. Pharmacol.* **161:** 1628–1644.
22. Abate, W., A. A. Alghaithy, J. Parton, K. P. Jones, and S. K. Jackson. 2010. Surfactant lipids regulate LPS-induced interleukin-8 production in A549 lung epithelial cells by inhibiting translocation of TLR4 into lipid raft domains. *J. Lipid Res.* **51:** 334–344.
23. Nakahira, K., H. P. Kim, X. H. Geng, A. Nakao, X. Wang, N. Murase, P. F. Drain, X. Wang, M. Sasidhar, E. G. Nabel, et al. 2006. Carbon monoxide differentially inhibits TLR signaling pathways by regulating ROS-induced trafficking of TLRs to lipid rafts. *J. Exp. Med.* **203:** 2377–2389.
24. Strandberg, Y., C. Gray, T. Vuocolo, L. Donaldson, M. Broadway, and R. Tellam. 2005. Lipopolysaccharide and lipoteichoic acid induce different innate immune responses in bovine mammary epithelial cells. *Cytokine.* **31:** 72–86.
25. Gilbert, F. B., P. Cunha, K. Jensen, E. J. Glass, G. Foucras, C. Robert-Granié, R. Rupp, and P. Rainard. 2013. Differential response of bovine mammary epithelial cells to Staphylococcus aureus or Escherichia coli agonists of the innate immune system. *Vet. Res.* **44:** 40.
26. Sordillo, L. M., and K. L. Streicher. 2002. Mammary gland immunity and mastitis susceptibility. *J. Mammary Gland Biol. Neoplasia.* **7:** 135–146.
27. Zheng, J., A. D. Watson, and D. E. Kerr. 2006. Genome-wide expression analysis of lipopolysaccharide-induced mastitis in a mouse model. *Infect. Immun.* **74:** 1907–1915.
28. Fernandez-Lizarbe, S., M. Pascual, M. S. Gascon, A. Blanco, and C. Guerri. 2008. Lipid rafts regulate ethanol-induced activation of TLR4 signaling in murine macrophages. *Mol. Immunol.* **45:** 2007–2016.
29. Janowski, B. A., M. J. Grogan, S. A. Jones, G. B. Wisely, S. A. Kliewer, E. J. Corey, and D. J. Mangelsdorf. 1999. Structural requirements of ligands for the oxysterol liver X receptors LXRalpha and LXRbeta. *Proc. Natl. Acad. Sci. USA.* **96:** 266–271.
30. Wang, N., M. Ranalletta, F. Matsuura, F. Peng, and A. R. Tall. 2006. LXR-induced redistribution of ABCG1 to plasma membrane in macrophages enhances cholesterol mass efflux to HDL. *Arterioscler. Thromb. Vasc. Biol.* **26:** 1310–1316.
31. Kennedy, M. A., G. C. Barrera, K. Nakamura, A. Baldan, P. Tarr, M. C. Fishbein, J. Frank, O. L. Francone, and P. A. Edwards. 2005. ABCG1 has a critical role in mediating cholesterol efflux to HDL and preventing cellular lipid accumulation. *Cell Metab.* **1:** 121–131.
32. Gelissen, I. C., M. Harris, K. A. Rye, C. Quinn, A. J. Brown, M. Kockx, S. Cartland, M. Packianathan, L. Kritharides, and W. Jessup. 2006. ABCA1 and ABCG1 synergize to mediate cholesterol export to apoA-I. *Arterioscler. Thromb. Vasc. Biol.* **26:** 534–540.